STUDIA UBB CHEMIA, LXV, 2, 2020 (p. 7-19)
(RECOMMENDED CITATION)
DOI:10.24193/subbchem.2020.2.01

THE EFFECT OF HALOGEN SUBSTITUTION ON THE BOWL-TO-BOWL INVERSION, MOLECULAR STRUCTURE AND ELECTRONIC PROPERTIES OF SUMANENE

AKIN AZIZOGLU[a,*], DUYGU EMIR[a]

ABSTRACT. Halogen (X: F, Cl, and Br) substituted sumanene derivatives were subjected to a detailed computational study, exploring the molecular structure, bowl-depths, bowl-to-bowl inversion dynamics, and electronic properties. Hybrid density functional (DFT, B3LYP, X3LYP and PBEKCIS) theoretical calculations were performed with an array of basis sets 6-31+G(d,p) and cc-pVTZ. The bowl shaped geometry and other properties were significantly affected by the introduction of halogens (F, Cl, and Br). Especially, the bond length alternations (Δ^1 *and* Δ^2) in the *hub* benzene ring and *flank* benzene ring of halogenated sumanenes (2Xa, 2Xb, and 12X) show remarkable sensitivity as a function of halogen with a wide range of fluctuations (0.011 to 0.071 Å). The introduction of fluorine to sumanene influences the bowl-to-bowl inversion energies slightly. The size of halogens seems to chiefly control the bowl depth and bowl-to-bowl inversion dynamic. In contrast, the bond length alternations seem to be controlled by electronic factors and not by the size of the substituted halogen atoms. The frontier molecular orbitals (FMOs) and molecular electrostatic potentials (MEPs) were significantly affected by the introduction of halogen atoms.

Keywords: *Sumanene, Halogens, Bowl-to-bowl inversion, DFT*

INTRODUCTION

The polycyclic aromatic hydrocarbons (PAHs) are formed by linear fusion and two dimensional growth of benzene [1]. Chemistry of nonplanar π-conjugated carbon molecules has received considerable attention in recent years due to their unique physical, chemical and assembling features [2]. They display unique properties such as bowl-to-bowl inversion, bowl chirality, electron conductivity, and columnar packing structure in the solid state [3].

[a] *Balıkesir University, Faculty of Arts and Sciences, Department of Chemistry, TR-10145, Balıkesir, Türkiye*
** Corresponding author: azizoglu@balikesir.edu.tr*

Buckybowls, also named π-bowls, are typical bowl-shaped aromatic hydrocarbons with open curved π-surface. Sumanene ($C_{22}H_{12}$, C_{3v}, Figure 1) is mainly derived from fullerene (C_{60}), composed of alternating benzenes and cyclopentadienes around the central benzene ring [1,4]. It can be defined as a piece of buckminsterfullerene with 21 carbon atoms and it poses both concave and convex π-surfaces with all vacant valences terminated by hydrogen [1,5]. Sumanene, a representative of the molecular π-bowls, has a bowl structure comprising five- and six-membered cycles. After the successful synthesis of sumanene in 2003, the interest in this compound increased and it has intensively been studied experimentally and theoretically [1-18].

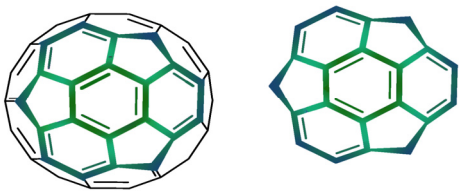

Figure 1. Fullerene (*left*) and Sumanene (*right*)

The bowl-to-bowl inversion is a distinctive character of some PAHs having π-bowl. Reported value of bowl-to-bowl inversion barrier for the sumanene is 16.9 kcal/mol employing B3LYP/cc-pVTZ//B3LYP/cc-pVDZ level of theory [6]. In the experimental works, bowl-to-bowl inversion barrier for sumanene is found to be ca. 20 kcal/mol (19.6 to 20.4 according to solvents) [7,8]. Theoretical and experimental findings suggest that sumanene is indeed rigid. Beside the bowl inversion energy barrier, it exhibited various unique properties such as columnar packing structure in the solid state [9], bowl chirality [10], electron conductivity [11], curved face-dependent stereoelectronic effect [12], and unprecedented coordination ability [13]. Among its interesting properties, Sakurai and et al. extensively studied the substituent effects on the bowl-to-bowl inversion and the correlation between the bowl structure and the bowl inversion energy by means of DFT calculation and experiments [14,15].

Sumanene also posed an appreciable challenge to synthetic chemists owing to its deep bowl depth. Many attractive properties have been studied since first successful synthesis of sumanene by Hirao and co-workers [8]. It has two different sides as concave (inside) and convex (outside) [16]. Furthermore, sumanene having three sp^3 hybridized carbon atoms at the benzylic positions is representative example of π-bowls [17. These benzylic positions of sumanene can allow the functionalization of new bowl shaped structure [18]. It is an enticing key structure that was examined by researchers for syntheses of novel bowl-forms [19].

Chemists regarding the influence of hetero-substitution of PAHs have also been extended to graphenes and nanotubes; properties like magnetism and mobility [20], sensing applications [21], electronic, aromatic and optical properties [22-25] have been studied.

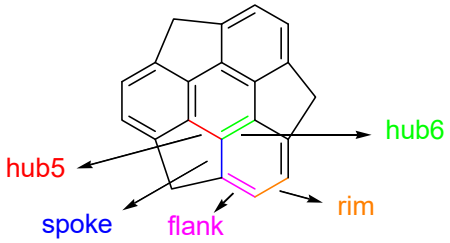

Figure 2. Different carbon bonds of sumanene

All these facts motivated us to investigate theoretically changes of essential properties of sumanene, the consequence of substitution of the aromatic and benzylic CH_2 groups with halogen atoms (F, Cl, and Br). We chose the DFT methods (B3LYP, X3LYP, and PBEKCIS) since this approach have proved to be a good solution when both accuracy and computational time are taken into account [26]. In this study, halogen (F, Cl, and Br) substituted sumanenes are considered for DFT-type calculations. Sumanene has five various C-C bonds, which include the *rim*, *flank*, *spoke*, *hub5* and *hub6*. For "*rim*" carbon atoms shown in Figure 2, three structures were obtained by replacing H with two halogen atoms (F, Cl, and Br). Other three ones were visualized by replacing H atoms of benzylic carbon atom with two halogen atoms. Last three compounds were modelled by substituting halogens (F, Cl, and Br) for all of H atoms of sumanene. The aim of the study was to get information about the selected geometric parameters, bowl depth, bowl-to-bowl inversion barriers, and electronic properties of nine sumanene derivatives by DFT treatments.

RESULTS AND DISCUSSION

After modelling the initial molecular structure of sumanene, its wide range of H atoms were replaced by fluorine, chlorine and bromine atoms, and nine different sumanene derivatives were obtained with the help of Gauss View 5.0 program. Three sumanenes were attained by substituting two halogen atoms for hydrogens at the "*rim*" carbon of sumanene (**2Fa, 2Cla, 2Bra**).

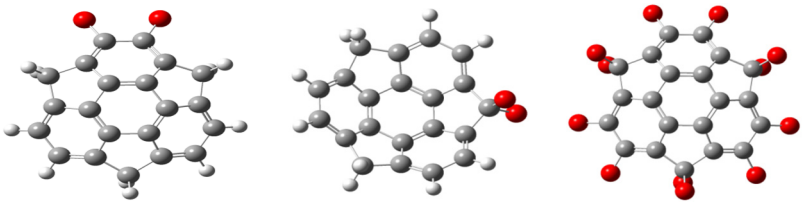

2Xa **2Xb** **12X**

Figure 3. Halogen (**X**: F, Cl, and Br) substituted sumanene derivatives subjected to theoretical calculations (**X**: red; Carbon: grey; Hydrogen: white colour)

Moreover, three sumanenes were achived by adding two halogens atoms to benzylic carbon of sumanene (**2Fb, 2Clb, 2Brb**). Finally, all hydrogen atoms of sumanene were substituted by halogen atoms (**12F, 12Cl, 12Br**), and thus three structures were obtained (Figure 3).

In the first part of the study, geometry optimizations of fluorine (**2Fa**, **2Fb**, **12F**), chlorine (**2Cla**, **2Clb**, **12Cl**), bromine (**2Bra**, **2Brb**, **12Br**) substituted sumanenes were performed at the (restricted) B3LYP/6-31+G(d,p), B3LYP/cc-pVTZ, X3LYP/6-31+G(d,p), X3LYP/cc-pVTZ, PBEKCIS/6-31+G(d,p) and PBEKCIS/cc-pVTZ levels. Then, their geometric parameters were calculated at the corresponding level of theories. The optmized geometries are virtually identical at all DFT levels. The Δ^1 and Δ^2 terms are formulated for the bond alternation of "*hub*" and "*flank*" benzene ring of halogen substituted sumanene, respectively.

$$\Delta^1 = r_{hub5} - r_{hub6} \quad (1)$$

$$\Delta^2 = r_{rim} - r_{hub6} \quad (2)$$

Bond alternations in the *hub* benzene ring (Δ^1) and *flank* benzene ring (Δ^2) of halogen (**X**: F, Cl, and Br) substituted sumanenes were given in Table 1. Lowest bond alternation is exhibited for the *hub* benzene ring of **2Bra,** where the electron-donating +I effect and electron-withdrawing –M effects are weak. This is in sharp contrast to the situation in the *hub* benzene ring of **12Cl**, which exhibits significant bond alternation. These results indicate that the electronic factors are chiefly responsible for bond length alternation. The bond alternations of **12F** in *hub* six-membered ring were calculated higher than *flank* ones. Similarly, bond variations in the *hub* of six-membered ring were calculated higher than *flank* six-membered ring for chlorinated sumanene except for **2Clb**. As it had been the same for the theoretical calculations made in advance, for brominated sumanenes, bond alternation in the *hub* of six-membered ring was calculated lower than *flank* position, and it is only the opposite for **12Br**. As indicated in Table 1 that the very slight

bond alternations of the *hub* and *flan*k benzene ring happened with the substitution of sumanene benzylic positions in all cases (**2Xbs**). Besides, improving the basis set quality further to 6-31+G(d,p) does not bring in any significant changes in the geometries and bond alternations.

Table 1. Bond alternations (Å) in the *hub* benzene ring (Δ^1) and *flan*k benzene ring (Δ^2) of fluorine, chlorine, and bromine substituted sumanenes at DFT levels.

	2Fa		**2Fb**		**12F**	
Theoretical Levels	Δ^1	Δ^2	Δ^1	Δ^2	Δ^1	Δ^2
B3LYP/6-31+G(d,p)	0.045	0.047	0.048	0.055	0.059	0.056
B3LYP/cc-pVTZ	0.049	0.049	0.049	0.057	0.061	0.058
X3LYP/6-31+G(d,p)	0.044	0.047	0.048	0.055	0.058	0.056
X3LYP/cc-pVTZ	0.048	0.049	0.049	0.057	0.061	0.058
PBEKCIS/6-31+G(d,p)	0.043	0.041	0.043	0.050	0.057	0.050
PBEKCIS/cc-pVTZ	0.047	0.042	0.044	0.051	0.060	0.052
	2Cla		**2Clb**		**12Cl**	
Theoretical Levels	Δ^1	Δ^2	Δ^1	Δ^2	Δ^1	Δ^2
B3LYP/6-31+G(d,p)	0.056	0.048	0.047	0.050	0.071	0.048
B3LYP/cc-pVTZ	0.057	0.049	0.047	0.051	0.070	0.050
X3LYP/6-31+G(d,p)	0.056	0.048	0.047	0.050	0.070	0.049
X3LYP/cc-pVTZ	0.057	0.049	0.047	0.052	0.070	0.050
PBEKCIS/6-31+G(d,p)	0.055	0.042	0.042	0.044	0.071	0.043
PBEKCIS/cc-pVTZ	0.055	0.043	0.042	0.046	0.070	0.044
	2Bra		**2Brb**		**12Br**	
Theoretical Levels	Δ^1	Δ^2	Δ^1	Δ^2	Δ^1	Δ^2
B3LYP/6-31+G(d,p)	0.012	0.047	0.044	0.047	0.066	0.046
B3LYP/cc-pVTZ	0.013	0.049	0.046	0.050	0.068	0.047
X3LYP/6-31+G(d,p)	0.012	0.048	0.044	0.047	0.065	0.046
X3LYP/cc-pVTZ	0.013	0.049	0.047	0.050	0.068	0.048
PBEKCIS/6-31+G(d,p)	0.011	0.041	0.042	0.044	0.064	0.041
PBEKCIS/cc-pVTZ	0.012	0.043	0.042	0.045	0.067	0.042

In the next part of the study, bowl depth (BD), depicted in Figure 4, was estimated for only three symmetrical compounds were obtained by substituting halogens (F, Cl, and Br) with all of H atoms of sumanene at the DFT levels studied herein. Bowl depth is known as the interplanar distance between the two planes formed by the central "*hub*" atoms and the "*rim*" carbon atoms [9,27,28].

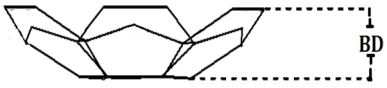

Figure 4. Bowl depth (BD)

Molecular bowl-depth of sumanene is equal to 1.11 Å in literature [13]. When examined the bowl depth values of halogenated sumanenes given in Table 2, the highest value of bowl depth for halogen substituted sumanene obtained by replacing hydrogen with fluorine atoms was calculated for **12F** compound at the PBEKCIS/6-31+G(d,p) level. **12F**s also have deeper bowl depths than the estimated value of unsubstituted sumanene (1.11Å). However, **12Cl**s and **12Br**s are slightly shallower than unsubstituted one. The lowest bowl depth was calculated to be 0.887 for **12Br** compound at the B3LYP/cc-pVTZ level. Calculated bowl depth values exhibited fluctuations according to the nature of halogen atoms.

Table 2. Bowl Depthes (BD) of twelve halogen substituted sumanene at DFT levels.

	BD (Å)		
Theoretical Levels	**12F**	**12Cl**	**12Br**
B3LYP/6-31+G(d,p)	1.133	0.922	0.896
B3LYP/cc-pVTZ	1.137	0.985	0.887
X3LYP/6-31+G(d,p)	1.140	0.930	0.900
X3LYP/cc-pVTZ	1.139	0.972	0.896
PBEKCIS/6-31+G(d,p)	1.142	0.987	0.926
PBEKCIS/cc-pVTZ	1.137	0.985	0.913

Then, bowl-to-bowl inversion barrier of studied molecules were estimated at the DFT levels. Bowl-to-bowl inversion activation energies ($\Delta E^{\#}$) including zero-point energy (ZPE) corrections (in kcal/mol), depicted in Figure 5, were calculated from the energy difference between the optimized bowl structure and the planar structure of sumanene as a transition state (**TS**) [2].

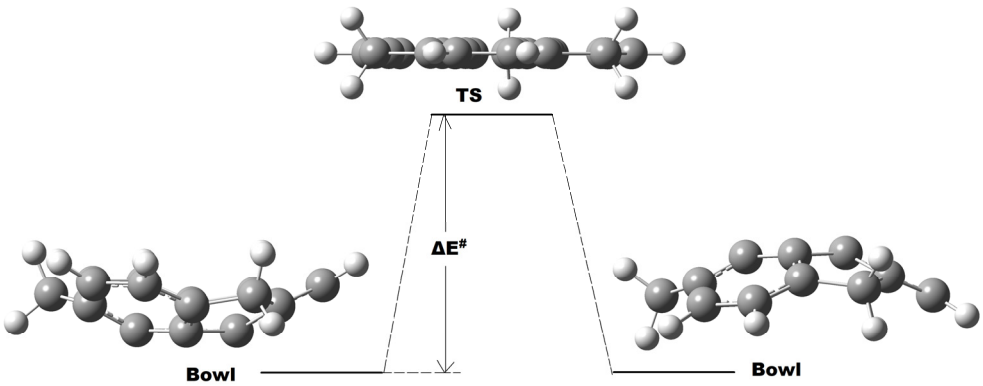

Figure 5. Schematic representation of the bow-to-bowl inversion barrier ($\Delta E^{\#}$, kcal/mol) for sumanene

All bowl-shaped compounds were structurally optimized at the beginning of the study. Then, their planar conformers for the transition states with one imaginary frequency were optimized at B3LYP/6-31+G(d,p), B3LYP/cc-pVTZ, X3LYP/6-31+G(d,p), X3LYP/cc-pVTZ, PBEKCIS/6-31+G(d,p) and PBEKCIS/cc-pVTZ levels. The normal mode corresponding to the one imaginary frequency had a direction corresponding to the bowl-to-bowl inversion process. Their IRC calculations linking planar transition structures to the bowl-shaped sumanenes were also performed to check the **TS** optimization procedures.

It can be easily understood from Table 3 that the highest bowl-to-bowl inversion energy barrier was obtained for **2Brb** as 21.3 kcal/mol at the PBEKCIS/6-31+G(d,p) level, whereas the lowest one was calculated to be 11.1 kcal/mol for **12Br** at the B3LYP/cc-pVTZ level.

Table 3. Bowl-to-bowl inversion barrier energy of fluorine, chlorine, and bromine substituted sumanene at DFT levels (ZPE included).

	$\Delta E^{\#}$ (kcal/mol)		
Theoretical Levels	**2Fa**	**2Fb**	**12F**
B3LYP/6-31+G(d,p)	17.3	18.7	16.6
B3LYP/cc-pVTZ	17.2	18.5	16.3
X3LYP/6-31+G(d,p)	17.5	18.9	17.1
X3LYP/cc-pVTZ	17.3	18.7	16.7
PBEKCIS/6-31+G(d,p)	18.0	19.3	16.1
PBEKCIS/cc-pVTZ	17.7	19.0	15.8
	2Cla	**2Clb**	**12Cl**
B3LYP/6-31+G(d,p)	17.9	18.6	13.7
B3LYP/cc-pVTZ	17.7	18.5	13.8
X3LYP/6-31+G(d,p)	18.1	18.8	14.1
X3LYP/cc-pVTZ	17.9	18.7	14.2
PBEKCIS/6-31+G(d,p)	18.8	19.3	14.0
PBEKCIS/cc-pVTZ	18.4	19.1	14.1
	2Bra	**2Brb**	**12Br**
B3LYP/6-31+G(d,p)	17.7	20.2	14.5
B3LYP/cc-pVTZ	17.6	18.3	11.1
X3LYP/6-31+G(d,p)	18.0	20.5	14.9
X3LYP/cc-pVTZ	17.8	18.6	11.4
PBEKCIS/6-31+G(d,p)	18.6	21.3	15.5
PBEKCIS/cc-pVTZ	18.4	19.0	11.8

Fluorinated sumanene derivatives exhibit slight changes in the bowl-to-bowl inversion energies at all DFT levels used herein. This is true for **2Cla** and **2Clb**, but the lower inversion barriers are computed for **12Cl**. It can be

also concluded in Table 3 that the slight increase of the bowl-to-bowl inversion barrier happened with the substitution of sumanene benzylic positions in all cases. However, the significant change occured with the substitution of all hydrogens of sumanene with bromine. These changes of the bowl-to-bowl inversion barrier are exclusively controlled by the size of the substituent and are independent of any electronic factors. Similar interpretations were reported by Armakovic and Sastry [7,27].

Compounds with non-linear optical (NLO) responses are of great importance as they find application in optical modulation, optical switching, optical logic, and optical memory for areas such as telecommunication, signal processing and optical interconnections [29,30]. Molecules having delocalized electrons have been observed to possess NLO properties. Hence, we have also undertaken to investigate the molecular orbitals of fully halogenated sumanenes (**12F**, **12Cl**, and **12Br**) with the help of the NBO analysis at the B3LYP/cc-pVTZ theory of level. As known that the relative orders of the highest occupied and lowest unoccupied molecular orbital (HOMO and LUMO, respectively) energies generally define conceivable qualitative indications of chemical stability, which are important criteria for developing organic semiconductor in electronic devices [31]. If the energy of HOMO is high, compounds may give electron more easily. It implies that NLO reactivity increases with rising of HOMO. The other parameter is the LUMO energy. If the E_{LUMO} value is lower, molecules may accept electrons and this result indicates that NLO reactivity of compounds increases with decreasing of E_{LUMO}. Electron mobility is important for reactivity determination. NLO activity increases with decreasing of the energy gap between frontier molecular orbitals (Δ_{gap} values). Theoretical LUMO-HOMO energy gaps also help characterize the chemical reactivity and the kinetic stability of the molecule. According to Fleming, a molecule having a small frontier orbital gap is more polarizable, and generally associated with a high chemical reactivity, low kinetic stability and also called as soft molecule [32-35]. It can be seen in Table 4 that unsubstituted sumanene has the biggest LUMO-HOMO energy gap with 7,74762 *eV*, whereas the **12Br** has the lowest one with 7,39475 *eV*. This smaller LUMO–HOMO gap means low excitation energies for many of excited states and low chemical hardness for **12Br**. The others, **12F** and **12Cl**, have 7,54197 and 7,40510 *eV* LUMO-HOMO gap values, respectively. According to E_{LUMO}, and Δ_{gap} values, **12Br** is the best one between of them in NLO activity except for the energies of HOMO. In other words, NLO activity may increase with the halogen substitution, especially bromine. Moreover, HOMO and LUMO orbitals are mainly on the double bonds, whereas HOMOs are substantially delocalized through the central benzene ring of **12F**, **12Cl**, and **12Br**. Electrons in the LUMO are also localized on the spoke, flank, and rim bonds.

Table 4. Energies of HOMO, LUMO, and Δ_{gap} (in *eV*) for **12F**, **12Cl**, and **12Br** at the B3LYP/cc-pVTZ level.

	Energies (*eV*)			
	Sumanene	**12F**	**12Cl**	**12Br**
LUMO	1.04709	-0.93907	-0.85417	-0.75403
HOMO	-6.70053	-8.48104	-8.25927	-8.14878
Δ_{gap}	7,74762	7,54197	7,40510	7,39475

The molecular electrostatic potential (MEP) map of studied molecules were calculated via electro-static potential (ESP) charges to determine their electron-deficient and electron-rich regions for nucleophlic and electrophilic attack, respectively. MEP maps, calculated at DFT B3LYP level of theory using cc-pVTZ basis set, are depicted in Figure 6.

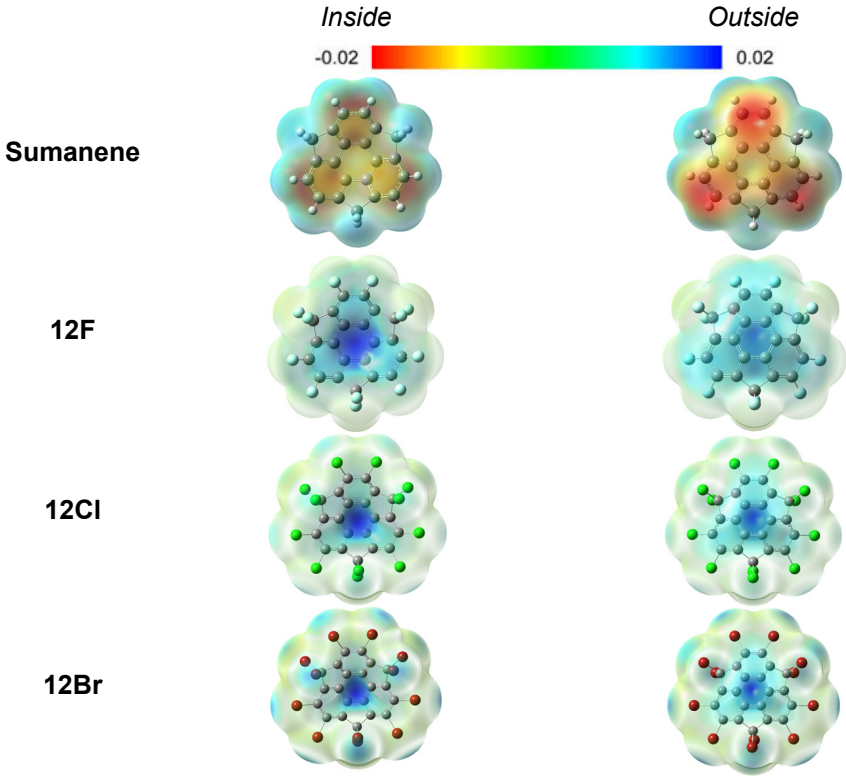

Figure 6. Molecular electrostatic potential maps of the title compounds

The negative (red colour) electrostatic potential regions of MEP were related to electrophilic reactivity and the positive (blue colour) ones to nucleophilic reactivity [36-38]. The regions with zero potential are represented in green. The electrostatic potential increases in the following order: red < orange < yellow < green < blue. The negative electrostatic potential signifies an attraction of the proton by the aggregate electron density in the compound (*shades of red*), and the positive electrostatic potential means the repulsion of the proton by the atomic nuclei (*shades of blue*).

The visualized MEP map depicts clearly that the negative electronic potential is found to be spread towards the concave and convex surface of sumanene; whereas the electronic potential is changed to neutral or even positive with the introduction of the electron-withdrawing halogen substituents. Upon substitution with halogen atoms the negative charge of the five and six membered rings is lost subsequently in the vicinity of halogens. The MEP surfaces on both faces of bowl of central benzene are nearly positive. Thus, it is confirmed that the electronic distribution of title sumanenes can be significantly affected by the presence of halogen substituents.

CONCLUSIONS

The molecular structure, bowl depth, bowl-to-bowl inversion, and electronic structure of the elusive key structural motif of halogenated sumanene are discussed using various density functional methods (B3LYP, X3LYP and PBEKCIS) with the 6-31+G(d,p) and cc-pVTZ basis sets for the first time. Sumanene derivatives were obtained by substitution of hydrogen atoms with fluorine, chlorine, and bromine atoms. The lowest bond alternation is found to be for the *hub* benzene ring of **2Bra,** where the electron-donating +I effect and electron-withdrawing –M effects are weak. However, the *hub* benzene ring of **12Cl** shows significant bond alternations. These results indicate that the electronic factors are chiefly responsible for bond length alternation of halogenated sumanenes. Moreover, improving the basis set quality further to 6-31+G(d,p) does not introduce any significant changes in the geometries and bond alternations of title molecules.

The fluorinated sumanenes (**12F**) have deeper bowl depths than unsubstituted sumanene (1.11Å), whereas the chlorinated (**12Cl**) and brominated (**12Br**) sumanenes are slightly shallower than unsubstituted one. Computed bowl depths at DFT levels exhibited fluctuations according to the nature of halogen atoms. Larger halogen atoms tend to flatten the structure and vice versa.

The lowest bowl-to-bowl inversion barrier is predicted to be 11.1 kcal/mol for **12Br** at the B3LYP/cc-pVTZ level including zero-point energy correction, whereas the highest one is calculated to be 21.3 kcal/mol for **2Brb** at the PBEKCIS/6-31+G(d,p) level. The introduction of fluorine to sumanene affect the bowl-to-bowl inversion energies slightly. Hence, the changes of the bowl-to-bowl inversion barrier are exclusively controlled by the size of the substituent and are independent of any electronic factors. The computational results indicate that halogenated sumanenes are not locked in the bowl geometry and that a bowl-to-bowl inversion could exist.

Moreover, the introduction of halogen substituents benefits the energetic stabilization of both the HOMO and LUMO. Lower values of the Δ_{gap} difference suggest a higher charge carrier mobility [39]. The π-electron-withdrawing halogens generally decrease Δ_{gap} of halogenated sumanene and these usually improve the carrier mobility of sumanene. The present theoretical results could be helpful for further studies on these interesting halogenated sumanenes.

EXPERIMENTAL SECTION

Computational details. The geometries of studied molecules were fully optimized with no symmetry constraints at the restricted B3LYP/6-31+G(d,p), B3LYP/cc-pVTZ, X3LYP/6-31+G(d,p), X3LYP/cc-pVTZ, PBEKCIS/6-31+G(d,p) and PBEKCIS/cc-pVTZ levels in the gas phase [40]. The geometries of title molecules were initially modelled by Gauss View 5.0 [41], and then the related theoretical calculations were done using the Gaussian 09W software [42]. Optimized structures were also checked using corresponding frequency calculations, which also used for calculating zero-point energy corrections (ZPE). Stationary points of outputs were defined as minima or transition structures by way of an analytic evaluation of harmonic vibrational frequencies at the level of geometry optimizations [43-46]. Moreover, the intrinsic reaction coordinates (IRCs) were pursued to prove the energy profiles relating each transition state to the correct local minima, by applying the second-order Gonzalez-Schlegel method [47].

ACKNOWLEDGMENTS

This research was supported by Balikesir University Scientific Research Projects Unit with the project number *2016-151* and *2016-156*. The authors would like to express their thanks to the reviewers for valuable comments that improved quality of the manuscript.

REFERENCES

1. D. Zhou; Y. Gao; B. Liu; Q. Tan; B. Xu; *Org. Lett.*, **2017**, *19*, 4628-4631.
2. T. Amaya; H. Sakane; T. Nakata; T. Hirao; *Pure Appl. Chem.*, **2010**, *82*, 969-978.
3. N. Ngamsomprasert; G. Panda; S. Higashibayashi; H. Sakurai; *J. Org. Chem.*, **2016**, *81*, 11978-11981.
4. T. Amaya; T. Hirao; *Chem. Record,* **2015**, *15*, 310-321.
5. E. Tahmasebi; Z. Biglari; E. Shakerzadeh; *Vacuum*, **2016**, *136*, 82-90.
6. U.D. Priyakumar; G.N. Sastry; *J. Phys. Chem.*, **2001**, *105*, 4488-4494.
7. S. Armaković; S.J. Armaković; J.P. Šetrajčić; I.J. Šetrajčić; *Chem. Phys. Lett.*, **2013**, *578*, 156-161
8. H. Sakurai; T. Daiko; T. Hirao; *Science*, **2003**, *301*, 1878-1878.
9. H. Sakurai; T. Daiko; H. Sakane; T. Amaya; T. Hirao; *J. Am. Chem. Soc.* **2005**, *127*, 11580−11581.
10. S. Higashibayashi; H. Sakurai; *J. Am. Chem. Soc.* **2008**, *130*, 8592−8593.
11. T. Amaya; S. Seki; T. Moriuchi; K. Nakamoto; T. Nakata; H. Sakane; A. Saeki; S. Tagawa; T. Hirao; *J. Am. Chem. Soc.* 2009, 131, 408−409.
12. S. Higashibayashi; S. Onogi; H.K. Srivastava; G.N. Sastry; Y.T. Wu; H. Sakurai; *Angew. Chem., Int. Ed.* 2013, 52, 7314−7316.
13. H. Sakane; T. Amaya; T. Moriuchi; T. Hirao; *Angew. Chem., Int. Ed.* **2009**, *48*, 1640−1643.
14. B.B. Shrestha; S. Karanjit; S. Higashibayashi; H. Sakurai; *Pure Appl. Chem.* **2014**, *86*, 747−753.
15. S. Higashibayashi; R. Tsuruoka; Y. Soujanya; U. Purushotham; G.N. Sastry; S. Seki; T. Ishikawa; S. Toyota; H. Sakurai; *Bull. Chem. Soc. Jpn.* **2012**, *85*, 450−467.
16. A. Reisi-Vanani; M. Hamadanian; S. N. Kokhdan; *Comput. Theor. Chem.*, **2016**. *1082*, 49-57.
17. T. Amaya; T. Ito; S. Katoh; T. Hirao; *Tetrahedron*, **2015**, *71*, 5906-5909.
18. S. Armaković; S.J. Armaković; J.P. Šetrajčić; *Int. J. Hydrog. Energy*, **2013**, *38*, 12190-12198.
19. A. Reisi-Vanani; S. Bahramian; *Comput. Theor. Chem.*, **2016**, *1093*, 40-47.
20. Y. Ma; A.S. Foster; A.V. Krasheninnikov; R.M. Nieminen; *Physical Review B*, **2005**, *72*, 205416.
21. K.P. Prathish; M.M. Barsan; D. Geng; X. Sun; C.M.A. Brett; *Electrochimica Acta*, **2013**, *114*, 533.
22. P. Nath; S. Chowdhury; D. Sanyal; D. Jana; *Carbon*, **2014**, *73*, 275.
23. M. Medeleanua; R. Pop; M. Andoni; *STUDIA UBB CHEMIA*, **2017**, *62(4)*, 105-119.
24. S. Armaković; S.J. Armaković; J.P. Šetrajčić; V. Holodkov; *J. Mol. Model.*, **2014**, *20*, 2538-2551.
25. X. Chen; F.-Q. Bai; Y. Tang; H.-X. Zhang; *J. Comput. Chem.*, **2016**, *37*, 813–824.
26. A. Karton; *J. Comput. Chem.*, **2016**, *38*, 370-382.

27. U.D. Priyakumar; G.N. Sastry; *J. Org. Chem.*, **2001**, *66*, 6523-6530.
28. Y. Sun; X. Hou; Chinese Chem. Lett., **2016**, *27*, 1166-1174.
29. V.M. Geskin; C. Lambert; J.L.Bredas; *J. Am. Chem. Soc.*, **2003**, *125*, 5651-15658.
30. D. Sajan; H. Joe; V.S. Jayakumar; J. Zaleski; *J. Mol. Str.*, **2006**, *785*, 43-53.
31. A. Rockett; Organic Semiconductors, in *The Materials Science of Semiconductors*, A. Rockett, Ed.; Springer, Boston, MA, **2008**, pp 395-453.
32. I. Fleming, "Frontier Orbitals and Org. Chemical Reactions", Wiley, London, **1976**.
33. Y. Tian; W. Chen; Z. Zhao; L. Xu; B. Tong; *J. Mol. Model.,* **2020**, *26*, 67.
34. L. Găină, I. Torje, E. Gal, A. Lupan, C. Bischin, R. Silaghi-Dumitrescu, G. Damian, P. Lönnecke, C. Cristea, L. Silaghi-Dumitrescu; *Dyes Pigments*, **2014**, *102*, 315.
35. A. Azizoglu; *Struct. Chem.*, **2003**, *14*, 575-580.
36. Z. Ozer, T. Kilic, S. Carikci, A. Azizoglu; *Russ. J. Phys. Chem. A*, **2019**, *93*, 2703–2709.
37. C.B. Yildiz; Z.O. Sagir; T. Kilic; A. Azizoglu; *STUDIA UBB CHEMIA*, **2014**, 59(2), 17-32.
38. S. Gosav; N. Paduraru; D. Maftei; M.L. Birsa; M. Praisler; *Spectrochim. Acta A*, **2017**, *172*, 115-125.
39. H. Unlu, *Solid State Electron*, **1992**, *35*,1343-1352.
40. D.C. Young; *Computational Chemistry*. New York, John Wiley & Sons Inc., **2001**, pp. 19-92.
41. R. Dennington; T. Keith; J. Millam; *GaussView*, **2009**, Version 5, Semichem Inc., Shawnee Mission KS.
42. M.J. Frisch; G.W. Trucks; H.B. Schlegel; G.E. Scuseria; M.A. Robb; J.R. Cheeseman; G. Scalmani; V. Barone; B. Mennucci; G.A. Petersson; H. Nakatsuji; M. Caricato; X. Li; H.P. Hratchian; A.F. Izmaylov; J. Bloino; G. Zheng; J.L. Sonnenberg; M. Hada; M. Ehara; K. Toyota; R. Fukuda; J. Hasegawa; M. Ishida; T. Nakajima; Y. Honda; O. Kitao; H. Nakai; T. Vreven; J.A. Montgomery Jr.; J.E. Peralta; F. Ogliaro; M. Bearpark; J.J. Heyd; E. Brothers; K.N. Kudin; V.N. Staroverov; R. Kobayashi; J. Normand; K. Raghavachari; A. Rendell; J.C. Burant; S.S. Iyengar; J. Tomasi; M. Cossi; N. Rega; J.M. Millam; M. Klene; J.E. Knox; J.B. Cross; V. Bakken; C. Adamo; J. Jaramillo; R. Gomperts; R.E. Stratmann; O. Yazyev; A.J. Austin; R. Cammi; C. Pomelli; J.W. Ochterski; R.L. Martin; K. Morokuma; V.G. Zakrzewski; G.A. Voth; P. Salvador; J.J. Dannenberg; S. Dapprich; A.D. Daniels; Ö. Farkas; J.B. Foresman; J.V. Ortiz; J. Cioslowski; D.J. Fox; *Gaussian 09*, revision *D.01*; Gaussian, Inc.: Wallingford, CT, 2009.
43. I.-T. Moraru, G. Nemes, *STUDIA UBB CHEMIA*, **2019**, *64(2)*, 435-446.
44. A.A. Attia; R.S. -Dumitrescu; *Int. J. Quant. Chem.*, **2014**, *114*, 652-665.
45. N. Azizoglu; M. Alkan; Ö. Geban; *J. Chem. Educ.*, **2006**, *83*, 947-953.
46. A. Azizoglu; R. Ozen; T. Hokelek; M. Balci; *J. Org. Chem.*, **2004**, *69*, 1202-1206.
47. C. Gonzalez; H.B. Schlegel; *J. Phys. Chem.*, **1990**, *94*, 5523-5527.